Continuous Radar-based Heart Rate Monitoring using Autocorrelation-based Algorithm in Intensive Care Unit

Sepehr Seifizarei, Ismail Elnaggar, Arman Anzanpour, Jonas Sandelin, Olli Lahdenoja, Miguel Glassee, Ivan D. Castro, Tom Torfs, Marcel CG van de Poll, Antti Airola, Matti Kaisti, Tero Koivisto

***Abstract*— This study presents a radar-based algorithm for non-invasive heart rate monitoring in intensive care units (ICUs) using a 140 GHz Frequency-Modulated Continuous Wave (FMCW) radar, placed unobtrusively beneath hospital beds. Data were collected from 15 post-operative cardiac patients at Maastricht University Hospital, with an ECG device serving as the ground truth for validation. The proposed algorithm includes data preprocessing, channel selection, heart rate estimation, and post-processing, employing autocorrelation to detect rhythmic patterns and quality metrics to ensure reliable channel selection. The system achieved a mean absolute error (MAE) of 2.22 beats per minute (bpm) with 66% overall coverage, increasing to 98% during sinus rhythm periods. This approach demonstrates robust performance in challenging ICU environments by mitigating noise and motion artifacts and optimizing computational efficiency. These findings highlight the potential of radar-based systems to enhance patient care through continuous, non-invasive vital sign monitoring and validate the algorithm's effectiveness in real-world clinical scenarios.**

***Index Terms*— Non-invasive, monitoring, radar, vital sign, heart rate, signal processing, intensive care unit (ICU), Bed monitoring**

I. Introduction

A. Background

INVESTIGATING physiological changes for early detection of abnormalities at home allows reducing hospitalization rates through early intervention. Classical approaches have had limited success in home monitoring due to the need to change the patient's habits or behavior as a significant barrier. However, recent developments in materials, devices, integrated electronic systems, and the Internet of Things (IoT) help address this issue specifically in diagnosing cardiovascular abnormalities [1].

Cardiovascular diseases (CVDs) are one of the most widespread and costly health problems people face today. CVDs are still the first global cause of morbidity and mortality, accounting for approximately 18.6 million deaths in 2019 [2], [3]. Consequently, the diagnosis and prevention of CVDs play a vital role in reducing the mortality and cost of CVD treatment [1], [4]. This matter requires continuous examination of the person's cardiovascular condition using bio-signals generated during the rhythmic heartbeat. Cardiovascular condition monitoring using radar is a relatively new field that has captivated attention in recent years due to the considerable developments in the design and manufacture of sensors that provide access to accurate measurements [5], [6], [7]. While these advancements hold promise for home monitoring applications, it is crucial to validate the technology in a controlled clinical environment first. Therefore, our study implements the radar detection system in a hospital setting, positioning it underneath the hospital bed to estimate heart rate.

B. Related Works

Traditional heart rate monitoring primarily relies on electrocardiography (ECG) sensors. These sensors offer high accuracy by directly measuring the electrical impulses generated by the heart. Photoplethysmography (PPG) offers another common approach, utilizing light to detect blood volume changes in tissues, which correlates with heart rate. Wearable devices often integrate these sensors due to their non-invasive nature and suitability for continuous monitoring applications [8]. While ECG and PPG excel in accuracy, they require physical contact with the body. Recent advancements have seen the introduction of ballistocardiography (BCG) sensors, which offer non-contact measurement by detecting the body's subtle movements caused by the heart's activity. However, BCG is less prevalent compared to ECG and PPG [9].

In contrast, radar-based monitoring presents a relatively new and promising approach for continuous, non-contact monitoring in both clinical and home settings. Several studies have explored the application of radar technology for physiological

Sepehr Seifizarei, Ismail Elnaggar, Arman Anzanpour, Jonas Sandelin, Olli Lahdenoja, Antti Airola, Matti Kaisti and Tero Koivisto are with the Department of Computing, the University of Turku, Turku 20500, Finland (e-mails: sepehr.seifizarei@utu.fi; ismail.m.elnaggar@utu.fi, arman.anzanpour@utu.fi, jojusan@utu.fi, olanla@utu.fi, mkaist@utu.fi, ajairo@utu.fi, tejuko@utu.fi). Miguel Glassee, Ivan D. Castro and Tom Torfs are with IMEC, 3001 Leuven, Belgium (e-mail: miguel.glassee@imec.be; ivand.castro@imec.be; tom.torfs@imec.be). Marcel CG van de Poll is with the Department of Intensive Care Medicine, Maastricht University Medical Center+, Maastricht, the Netherlands; School for Nutrition and Translational Research in Metabolism (NUTRIM), Maastricht University, Maastricht, the Netherlands (e-mail: marcel.vande.poll@mumc.nl).

monitoring in diverse environments. Qiao et al. [10] demonstrated the successful extraction of respiration and heart rates from stationary participants using continuous-wave Doppler radar, validating its accuracy against ECG monitors. Xu et al. [11] further explored this concept by employing ultra-wideband radar to accurately detect heart and respiration rates, emphasizing its robustness under various bed positions and body angles. Additionally, Huang et al. [12] developed a self-calibrating radar sensor system for reliable vital sign measurement across multiple experimental setups.

Li et al. [13] demonstrated the feasibility of non-contact respiration and heartbeat monitoring using microwave Doppler radar, highlighting its potential for remote vital sign detection. Khan and Cho [14] addressed the challenge of separating heart rate signals from breathing harmonics by developing an algorithm specifically for vital sign monitoring using impulse radio ultra-wideband radar. Singh et al. [15] provided a comprehensive review, discussing the advancements and challenges of non-contact vital sign monitoring using radar, emphasizing the need for higher frequencies to improve accuracy, particularly in multi-resident environments. Schellenberger et al. [16] explored a multi-radar setup for continuous in-bed monitoring of vital signs, allowing for unobtrusive monitoring of freely moving participants. Finally, Paterniani et al. [17] provided a tutorial overview of radar-based vital sign monitoring, including guidelines for selecting radar devices and signal processing algorithms.

Our study builds on and advances the existing body of research by addressing the challenges of radar-based monitoring in dynamic clinical environments, specifically intensive care units (ICUs), where patient movement and environmental noise present unique obstacles. Our proposed system integrates radar technology beneath the hospital bed, providing continuous, non-invasive monitoring of heart rate in ICU settings. This unobtrusive placement eliminates the need for physical contact, improving comfort and reducing the risk of infection. Unlike previous studies that focus on stationary or controlled environments, our system adapts to ICU conditions, using advanced signal processing techniques to filter noise and maintain high accuracy under movement and noise disturbances.

Additionally, our approach is clinically validated on patients recovering from cardiovascular surgeries, offering significant relevance compared to studies focusing solely on healthy individuals. Qiao et al. [10] utilized continuous-wave Doppler radar for stationary participants, demonstrating the potential of radar in controlled environments. In contrast, our system is designed for ICU settings, where patient movement is common, and leverages Frequency-Modulated Continuous Wave (FMCW) radar to provide enhanced distance measurement capabilities. Similarly, Xu et al. [11] emphasized robustness across varying bed angles using ultra-wideband radar. Our approach builds on this robustness while improving detection accuracy with advanced signal processing tailored to the noisy ICU environment. Furthermore, unlike Huang et al. [12], who proposed a self-calibrating radar sensor, our system prioritizes patient comfort through a non-invasive, under-bed installation, enhancing usability in clinical settings.

In summary, our proposed system integrates advancements in signal processing and practical deployment, tailored specifically for ICU settings. This paper is structured as follows: Section II describes the sensor setup, data acquisition process, and algorithm development, including quality assessment, heart rate estimation, and post-processing techniques. Section III presents the evaluation of the algorithm's performance, showcasing statistical results and visual analyses. Section IV provides a detailed discussion of the findings, including a comparison with recent radar-based heart rate monitoring methods. Finally, Section V concludes the study by summarizing the contributions and outlining potential future research directions.

II. Materials and Methods

An overview of the proposed method, from data acquisition to heart rate estimation, is shown in Figure 1.

A. Sensor Configuration

In this study, we utilized a FMCW MIMO Radar, specifically the "WiSens" 140 GHz radar sensor developed by IMEC, Belgium [18]. The high center frequency and high bandwidth used by this radar make it suitable for applications requiring fine-grain range resolution and accurate velocity detection.

Figure 1 displays the ECG and radar devices used for data recording and their integration within the heart rate estimation workflow.

The WiSens radar operates at a center frequency range of 140 GHz and utilizes a modulation bandwidth of 10 GHz. It is designed to operate efficiently with a typical power consumption of 9W. The radar module itself is compact, with dimensions of 110 mm x 110 mm x 46mm, and weighs 620 grams. The radar's range resolution is 1.49 cm. For this study, it was configured as a linear array using 2 transmit antennas and 2 receive antennas. This allows focusing the detection to the plane perpendicular to the radar, reducing potential interference from persons or equipment standing next to the bed. The radar and its capturing software were configured to capture 32 range bins starting from 10.42 cm up to 58.04 cm in front of the radar. Doppler processing and low-pass filtering where configured to obtain a signal with a sampling frequency of 207.78 Hz.

The integration of the radar module into the hospital bed setup involved mounting it beneath the bed using a custom-designed bracket that ensures stability and optimal alignment with the patient's chest area, without limiting the possible positons of the bed. Considering a range of mattress compression, the radar module was positioned to point towards the patient's chest, ensuring the patient's back would fall within its detectable range. For patient safety and prevent interference with other medical equipment, the radar module's housing is designed to limit exposure to radio waves except for the antenna, which needs a clear path to transmit and receive signals. Regular maintenance checks are conducted to ensure the module functions correctly. The field strength of

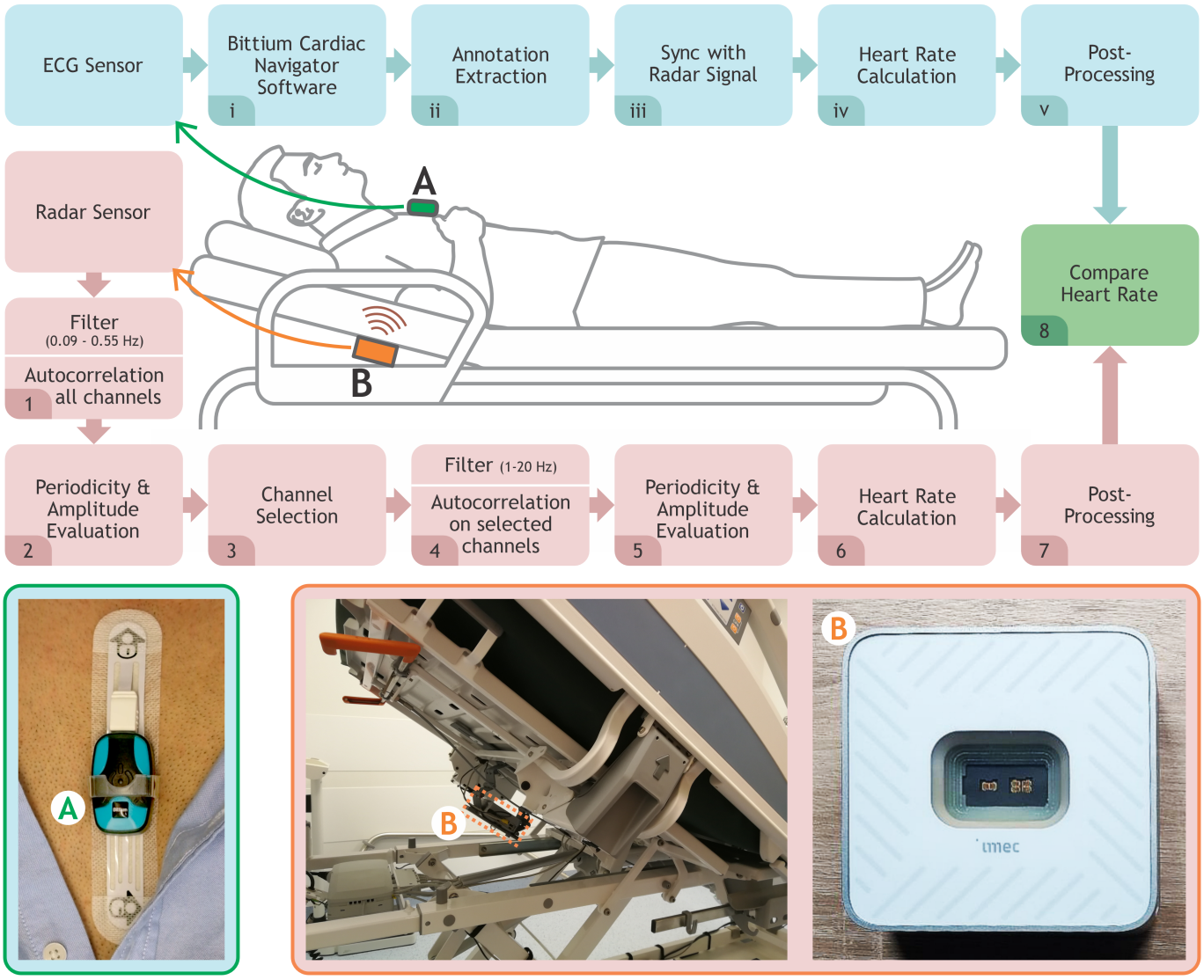

Fig. 1: Overview of the proposed method for heart rate estimation from radar and ECG data, including sensor configuration, data acquisition, signal processing, and heart rate calculation steps. Two main devices are used: (A) the Bittium Faros Holter monitor for ECG and (B) the IMEC radar module for radar data. The radar device and associated processes are shown in the red-shaded background, while the ECG device and its process flow are displayed in the blue-shaded background.

the electromagnetic field emitted by the radar is sufficiently low to guarantee patients and hospital workers safety.

Additionally, Bittium Faros Holter monitor is used as a reference. It stores ECG signal data on its internal memory. These signals are later merged during the analysis phase using their common initially-synced sampling timestamps. The ECG reference signals are analyzed for the extraction of cardiac rhythms via the Bittium Cardiac Navigator™, a clinical, FDA-approved, and CE-certified Holter ECG analysis software.

B. Data Collection

Data for this study were collected from 15 patients at Maastricht University Hospital as part of the Moore4Medical Project, using various sensor combinations. Radar data was unobtrusively gathered by placing the radar module beneath hospital beds, enabling continuous monitoring without disturbing the patients. All patients were post-operative, recovering from different cardiac surgeries and procedures. This setup provided a realistic clinical environment to assess the radar system's effectiveness in detecting heart rates in individuals with cardiovascular conditions.

Table I presents the summary statistics of the demographic data for patients population, including age, weight, height, Body Mass Index (BMI), and sex.

TABLE I: Summary statistics of patients' demographic data.

Age	Height [cm]	Weight [kg]	BMI	Sex [M/F]
64 ± 9.6	172 ± 6.6	82 ± 14.2	28 ± 4.1	11/4

This dataset is particularly unique due to two main factors.

First, the data was collected in an ICU setting, which provides a realistic and practical context for the data. Second, the extensive duration of recordings, with some patients providing continuous data for nearly two days, allows for a more comprehensive assessment of patients health and activity.

The study protocol was reviewed by the Medical Ethical Committee of University Hospital Maastricht/Maastricht University who judged that the Medical Device Regulation (MDR) and the Medical Research Involving Human Subjects Act (WMO) do not apply (METC2022-3188). All patients provided written informed consent.

C. Algorithm Description

The proposed algorithm for detecting vital signs utilizes autocorrelation and comprises several key steps: quality assessment, data preprocessing, channel selection, heart rate estimation, and post-processing. Figure 1 provides an overview of the complete method, from data acquisition to heart rate estimation, while the pseudocode specifically for the heart rate estimation algorithm is outlined in Algorithm 1.

1) Quality Assessment: Considering the non-invasive nature of radar signals, data quality can vary significantly based on patient movement and positioning [19]. To ensure the accuracy and reliability of the estimated heart rates, two criteria are checked during the calculation step to select channels with high-quality signals:

1) **Autocorrelation Periodicity Percentage:** This metric evaluates the consistency of detected peaks within the autocorrelation function. We calculate this percentage by considering the variability of peak intervals. Specifically, we take into account the typical range of human respiration rates (maximum respiratory rate variability of 2 seconds) [20] and heart rates (maximum heart rate variability of 200 milliseconds) [21]. A higher periodicity percentage indicates more consistent peak timing, suggesting a stronger presence of a repetitive pattern in the radar signal.
2) **Autocorrelation Amplitude Change Percentage:** This metric evaluates the level of non-repetitive noise within the radar signal. We calculate the change in amplitude between the first and second detected peaks of the autocorrelation function. A higher amplitude change indicates the presence of more significant non-repetitive noise components.

If a channel's periodicity percentage is over 70% and its amplitude change percentage is below 50%, the signal quality is deemed sufficient.

2) Data Preprocessing: To extract vital signs, the complex raw radar data is first converted into displacement signals. This conversion simplifies further analysis and reduces computational demands by transforming the received radar signals into a format that represents the displacement of the chest caused by respiration and heartbeat. This is done by analyzing the phase shift of the received signal relative to the transmitted signal, which directly correlates with the displacement of the target (i.e., the chest). The phase change information is obtained by transmitting multiple chirps and ensuring the phase change occurs between two chirps or frames, which allows for accurate displacement measurement [14]. Given the disparate collection devices, ECG and radar signals are synchronized based on the starting timestamps of each recording, facilitating comparative and precise analysis. For channel selection, the radar signal is divided into 30-second segments and filtered using a 2nd order Butterworth band-pass filter with cut-off frequencies set between 0.09 and 0.55 Hz to eliminate signal noise [22]. To estimate heart rate with improved accuracy and isolate potential heartbeats within the signal, the signal is further segmented into 10-second intervals with 5 seconds of overlap. This overlapping window technique allows for a more continuous analysis and reduces the risk of losing data at the interval boundaries [23]. Additionally, each segment is filtered with cut-off frequencies between 1 Hz and 20 Hz

Algorithm 1 Radar-based heart rate estimation algorithm

Input: $\mathbf{D} \in \mathbb{R}^{N\times 32}$ (Radar Displacement Signal, N: time samples, 32: range bins)
Output: $\mathbf{HR}_{\text{final}} \in \mathbb{R}^{M}$ (M: number of 10-second mini-segments)

// Remove noise and irrelevant frequencies.
$\mathbf{D}_{\text{filtered}} \leftarrow$ Band-pass-Filter$(\mathbf{D})$
// Segment into 30-second segments.
$\mathbf{S} \leftarrow$ Segment$(\mathbf{D}_{\text{filtered}}, 30)$
// Initialize array for mini-segment HR values.
$\mathbf{HR}_{\text{mini}} \leftarrow \emptyset$
// Initialize array of all range bin indices
$\mathbf{B} \leftarrow \{1, 2, \ldots, 32\}$
// Initialize dynamic structure to store peaks.
$\mathbf{P1} \leftarrow$ empty dictionary
for $i \leftarrow 1$ to $|\mathbf{S}|$ **do**
  for $j \leftarrow 1$ to $|\mathbf{B}|$ **do**
    // Calculate autocorrelation for segment i and range bin j.
    $\mathbf{A}_{ij} \leftarrow$ Autocorr$(\mathbf{S}_i, j)$
    // Detect an array of peak locations in the autocorrelation signal.
    $\mathbf{P1}[(i,j)] \leftarrow$ Detect-Peaks$(\mathbf{A}_{ij})$
  end for
  // Select range bins based on quality metrics.
  $\mathbf{B}_{\text{selected}} \leftarrow \{j \in \mathbf{B} : \text{Periodicity}(\mathbf{P1}[(i,j)]) > 70\% \wedge \text{AmplitudeChange}(\mathbf{P1}[(i,j)]) < 50\%\}$
  if $|\mathbf{B}_{\text{selected}}| \geq 3$ **then**
    // Segment into 10-second mini-segments with 5-second overlap.
    $\mathbf{M} \leftarrow$ Segment$(\mathbf{S}_i, 10, \text{overlap} = 5)$
    // Initialize dynamic structure to store peaks for mini-segments
    $\mathbf{P2} \leftarrow$ empty dictionary
    for $k \leftarrow 1$ to $|\mathbf{M}|$ **do**
      for $l \leftarrow 1$ to $|\mathbf{B}_{\text{selected}}|$ **do**
        // Calculate autocorrelation for mini-segment k and range bin l.
        $\mathbf{A}_{kl} \leftarrow$ Autocorr$(\mathbf{M}_k, l)$
        // Detect peaks in the autocorrelation signal.
        $\mathbf{P2}[(k,l)] \leftarrow$ Detect-Peaks$(\mathbf{A}_{kl})$
        // Compute HR based on peak intervals.
        $\mathbf{HR}_{kl} \leftarrow$ CalculateHR$(\mathbf{P2}[(k,l)])$
      end for
      // Calculate the median HR for the mini-segment k.
      $\mathbf{HR}_k \leftarrow$ Median$(\{\mathbf{HR}_{kl}\})$
    end for
    // Store HR value of mini-segment k.
    $\mathbf{HR}_{\text{mini}} \leftarrow \mathbf{HR}_{\text{mini}} \cup \{\mathbf{HR}_k\}$
  end if
end for
// Apply a median filter over 60 seconds to smooth the results.
$\mathbf{HR}_{\text{baseline}} \leftarrow$ MedianFilter$(\{\mathbf{HR}_{\text{mini}}\}, \text{window} = 11)$
// Filter out HR values deviating by more than 16 BPM from the baseline.
$\mathbf{HR}_{\text{final}} \leftarrow \{\mathbf{HR}_{\text{mini}} : |\mathbf{HR}_{\text{mini}} - \mathbf{HR}_{\text{baseline}}| \leq 16\}$
return $\mathbf{HR}_{\text{final}}$

correspond to the typical human heart rate range. The lower limit of 1 Hz is equivalent to 60 beats per minute (bpm), ensuring that lower heart rates are not excluded from analysis. The upper limit of 20 Hz helps to maintain the sharpness of the heartbeat signals, preventing the loss of detailed information about each beat and minimizing the impact of high-frequency noise [24]. Furthermore, the use of a second-order Butterworth filter ensures a smooth transition within the passband, allowing for the inclusion of slightly lower heart rates than 60 bpm due to the filter's gradual attenuation characteristic [25]. This characteristic ensures that the stopband does not sharply exclude lower frequencies, providing a more inclusive analysis for lower heart rates.

3) Channel Selection: To ensure reliable heart rate results, only high-quality channels (range bins) are considered for further analysis. Since respiration movements are easier to detect in radar signals compared to subtle heart movements, we prioritize channels where respiration rates were successfully estimated. The selection process involves applying the autocorrelation function to 30-second signal segments. This function emphasizes rhythmic patterns, facilitating the identification of peaks within the signal. Respiration rates are then calculated for each channel based on the intervals between these detected peaks. Finally, only channels that satisfy both quality criteria (described previously) and exhibit a respiration rate within the normal human range of 10 to 20 breaths per minute are selected for heart rate estimation. By focusing on channels with confirmed respiratory activity and applying these quality filters, the selection process enhances the accuracy and reliability of subsequent heart rate estimations.

4) Heart Rate Estimation: For each channel selected in the previous stage, we calculate the autocorrelation of 10-second signal segments. This function again emphasizes rhythmic patterns, but with a focus on the faster timescale relevant to heart rate. The heart rate for each channel is then estimated based on the intervals between the detected peaks in the autocorrelation signal. To enhance robustness and minimize the influence of outliers, the final heart rate is determined as the median value across all channels that met the quality criteria. This median is only calculated if at least three channels qualify, ensuring sufficient data for a reliable estimate.

5) Post-processing: To further refine the heart rate estimates and eliminate potential outliers, a median filter is applied as a post-processing step. This filter operates on a window of 11 data points, corresponding to a window duration of 60 seconds. It identifies and removes outliers by eliminating values that deviate significantly from the median baseline within the window. The threshold for this deviation is set at 16 beats per minute, as described in [26].

It is important to note that this post-processing step may inadvertently filter out abnormal heart rates, such as those occurring during arrhythmias. While the primary focus of this study is on accurate heart rate detection, the unperiodic nature of arrhythmias leads to these segments being classified as low quality and excluded by the channel selection criteria. This approach enhances the reliability of heart rate estimation for the intended use case but may limit the system's current utility in detecting and monitoring arrhythmias. This trade-off is acknowledged in the context of the intended clinical use case.

Figure 2 illustrates the effectiveness of this post-processing step. It shows the estimated heart rates for patient 15 using a radar signal, both before and after applying the median filter. The figure visually demonstrates how outliers are eliminated, leading to a smoother and more reliable heart rate estimation.

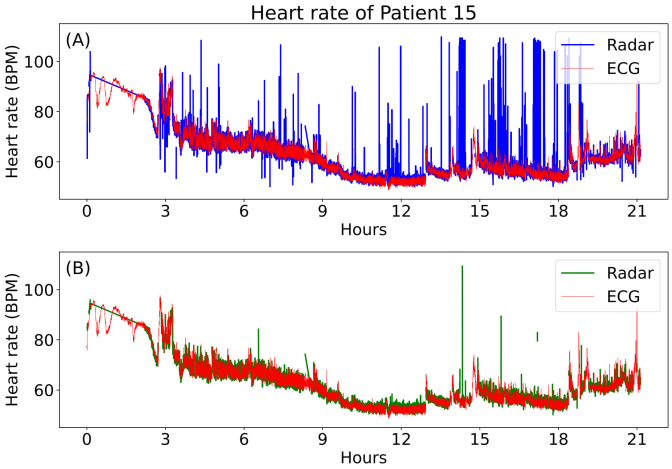

Fig. 2: An example of calculated heart rates before (A) and after (B) the post-processing step. The red line represents the actual heart rate measured by ECG, providing a ground truth reference. The blue line depicts the initial estimates obtained from the radar signal. The green line shows the final, more reliable heart rate values after applying the median filter during post-processing.

III. Results

In this section, we present the results and findings obtained from the evaluation of our proposed algorithm for bed monitoring using radar sensors. Key aspects of the algorithm's performance are assessed, including accuracy, coverage, and the impact of quality assessment on heart rate detection.

First, we analyze the results of the algorithm for all patients using the default settings described in the previous sections.

Table II presents the overall performance of the proposed algorithm, including metrics such as total recording duration, mean absolute error (MAE), coverage, and median heart rates from both ECG and radar data.

During our analysis, we tracked both the total number of segments processed by our algorithm and the segments excluded or ignored based on quality control criteria. This enabled us to calculate the algorithm's total coverage percentage over the entire recording duration for each patient. Despite the radar signal's high sensitivity to motion artifacts and patients' body positions, we found an average coverage percentage exceeding 66%. This is notable considering that 26% of the total recordings involved patients experiencing various types of arrhythmias. These findings demonstrate the proposed

TABLE II: Summary of heart rate monitoring results.

Patient ID	Total Record Duration (mins)	MAE (bpm)		Coverage (%)		ECG HR Median (bpm)	ECG HR STD (bpm)	Radar HR Median (bpm)		Radar HR STD (bpm)		Sinus Rhythm Ratio (%)
		Before[1]	After[2]	Before[1]	After[2]			Before[1]	After[2]	Before[1]	After[2]	
1	2195	11.16	5.35	95.89	50.49	73.44	24.39	65.96	70.83	18.41	8.96	60.7
2	998	12.85	4.93	98.59	38.77	79.37	11.21	55.65	79.40	14.84	9.99	3.8
3	1159	3.20	1.17	99.40	70.87	69.44	6.20	67.75	69.25	13.81	4.00	81.5
4	1254	5.51	1.30	99.05	80.76	95.39	8.09	86.64	96.63	20.11	7.92	97.7
5	2315	10.43	3.28	99.45	70.39	88.76	7.21	82.28	87.78	20.95	8.12	82.1
6	1055	6.17	3.02	97.90	51.01	62.57	7.18	62.64	61.71	19.31	6.26	84.9
7	17	1.08	1.08	98.69	84.72	60.09	1.22	58.25	59.64	6.46	2.36	80.8
8	350	3.84	0.97	98.74	73.86	89.55	2.05	88.01	90.00	19.75	2.17	37.8
9	1349	8.23	3.11	98.74	47.90	74.91	10.31	64.86	74.98	21.55	9.52	91.1
10	254	2.39	0.36	97.56	76.03	80.00	0.94	79.91	79.91	25.18	0.99	97.0
11	1266	6.06	3.09	98.35	45.54	67.95	8.00	57.07	66.84	15.70	6.10	86.4
12	1150	3.05	1.11	96.05	64.23	69.77	9.51	67.07	70.43	16.42	9.32	79.1
13	79	1.06	0.56	99.07	85.46	76.53	2.75	76.71	77.07	12.35	2.51	40.3
14	1197	6.82	2.31	98.35	67.80	79.68	6.16	75.09	78.40	16.32	5.61	88.3
15	1188	1.95	1.65	98.51	84.23	61.35	11.29	58.66	59.43	10.85	7.57	97.9
Mean	15825	5.59	2.22	98.29	66.14	75.25	7.77	69.77	74.82	16.80	6.09	74.0

[1] Metrics calculated before channel selection. [2] Metrics calculated after channel selection.

algorithm's effectiveness in processing continuous patient data in real-life scenarios.

We assessed the impact of the channel selection step on the accuracy of heart rate detection, using the ECG signal as the reference. The resulting changes in Mean Absolute Error (MAE), coverage, as well as the median and standard deviation of the calculated radar heart rate (HR), are presented in separate columns labeled "Before" and "After" in Table II.

Initially, heart rate detection showed a wider range of error values due to the influence of noise and the inclusion of less relevant range bins. After applying the channel selection step, the MAE was reduced by an average of 60%.

We also noted a significant impact of signal quality fluctuations on the algorithm's coverage percentage. These fluctuations are often linked to heart arrhythmias such as atrial fibrillation and ectopic heartbeats, which are typically non-periodic. As a result, the autocorrelation from these segments cannot be used for heart rate estimation due to the low quality according to defined quality metrics.

While this limitation prevents the algorithm from accurately estimating heart rate during arrhythmic episodes, monitoring heart rate trends during non-arrhythmic periods still provides significant clinical value. To evaluate the algorithm's performance under more stable conditions, we focused on segments occurring during sinus rhythm, excluding those marked by arrhythmias. This analysis showed a marked improvement, with average coverage exceeding 98%. These findings demonstrate the algorithm's capability for reliable and continuous heart rate monitoring, underscoring its potential as a valuable tool for real-world applications and extended patient observation scenarios where precise and stable monitoring conditions are crucial. Figure 3 illustrates an example of the algorithm's coverage during different heart rhythms.

Additionally, to evaluate the agreement between the heart rate measurements obtained from the radar system and the ECG, we utilized a Bland-Altman plot. As shown in Figure 4, the plot illustrates the differences between the heart rate measurements (HR_{ECG} - HR_{RADAR}) against their average values. The dashed lines indicate the mean difference and the 96% limits of agreement, providing a visual representation of the agreement between the two measurement methods. The majority of the differences fall within the 96% limits, indicating good agreement between the radar-based heart rate detection and the ECG reference standard.

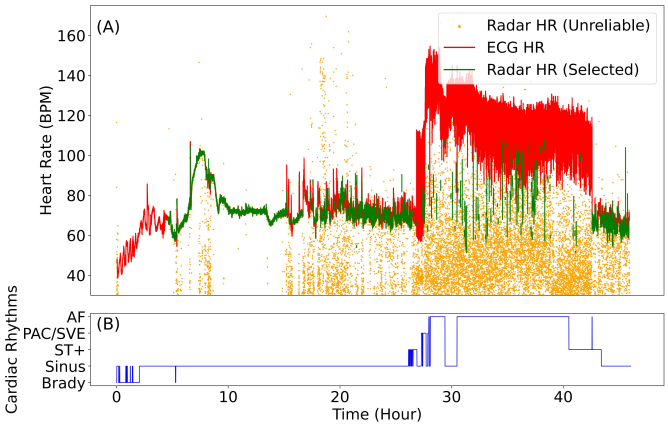

Fig. 3: The algorithm coverage along with cardiac rhythm change during the recording of patient No. 1. The top plot (A) shows the algorithm results for the whole measurement in which green points are the final estimated heart rates and the orange points show unreliable heart rates. The below plot (B) shows the change in cardiac rhythm during the measurement, which is extracted using Bittium Cardiac Navigator software.

To further understand the performance of the proposed algorithm, we used heatmaps to visualize the selection and effectiveness of radar range bins. These analyses provide a detailed view of how different range bins contribute to the channel selection and overall heart rate detection. Heatmap plots (Figure 5 and Figure 6) illustrate the distribution of selected radar range bins for both channel selection based on respiration rate and heart rate detection across all patients. The brighter-colored cell blocks indicate a higher percentage of selection, signifying more reliable signal detection at those specific range bins.

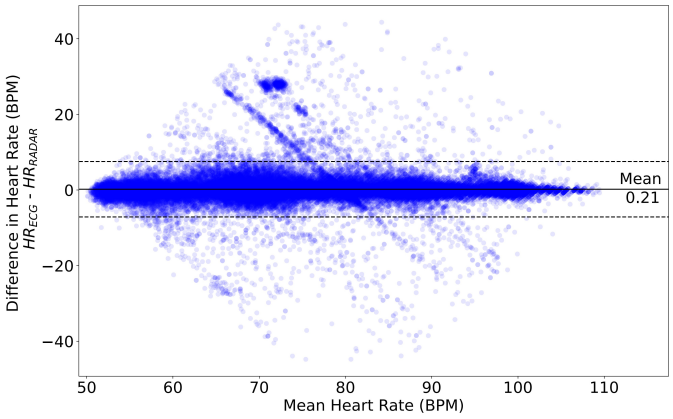

Fig. 4: Bland-Altman plot comparing the heart rate measurements from the radar system and ECG. The plot shows the difference in heart rate (HR_{ECG} - HR_{RADAR}) against the mean heart rate (bpm). The dashed lines represent the mean difference and the 96% limits of agreement.

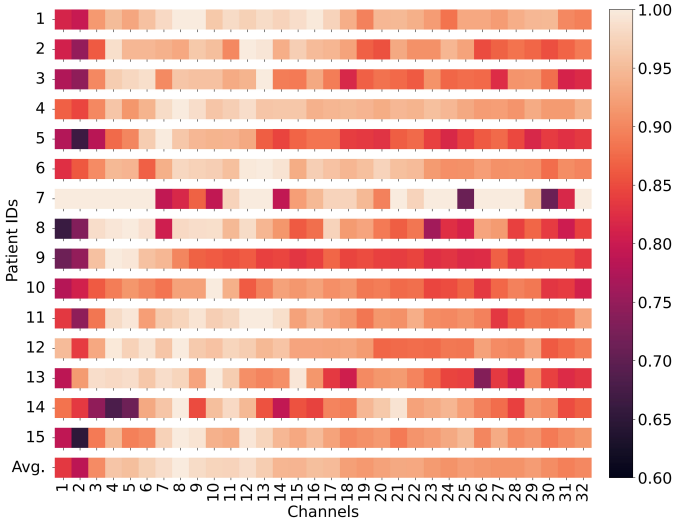

Fig. 5: Distribution of selected radar range bins for channel selection across all patients.

Figure 5 illustrates a broader range of bins selected during the respiration rate detection step, spanning across most of the 32 radar range bins. This broad selection indicates that respiration-related movements, such as chest expansions, are detectable over a wider range of the body and bed area. This diversity provides multiple high-quality signals, improving the robustness of respiration rate estimation and facilitating further channel selection.

In contrast, Figure 6 demonstrates that heart rate detection predominantly relies on the first 16 range bins, which correspond to radar channels closest to the sensor, covering a distance range from approximately 10.42 to 33.26 cm from the radar module. This concentration indicates that heart-related movements are more localized, allowing the algorithm to focus on fewer, but higher-quality, signals for heart rate estimation.

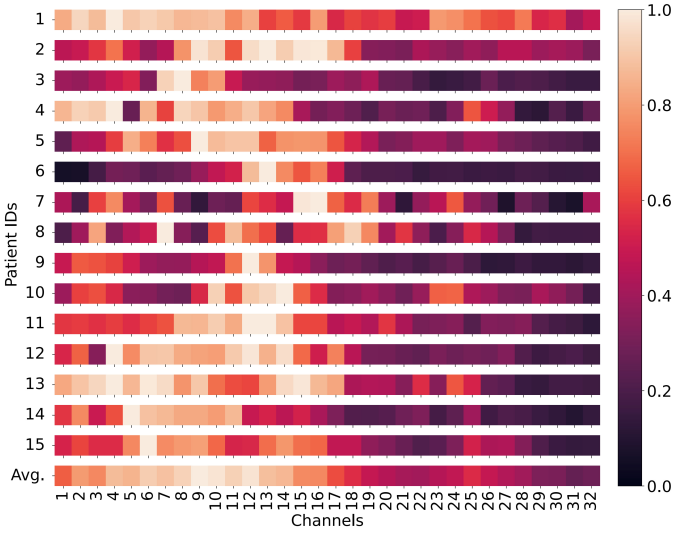

Fig. 6: Distribution of selected radar range bins for heart rate detection across all patients.

IV. Discussion

In this paper, we introduced a radar-based algorithm for bed monitoring, specifically for heart rate estimation, validated in real-world ICU settings. Using data from post-surgical patients recovering from cardiovascular interventions, our approach demonstrated robustness, achieving low error rates even with challenges such as motion artifacts and patient positioning variations. These results affirm the system's reliability and clinical applicability.

Our findings suggest that this radar-based monitoring system can enhance patient care by providing continuous, non-invasive monitoring, reducing the need for manual measurements, and increasing patient comfort. The under-bed placement of the radar minimizes interference with clinical workflows, enhances patient comfort, and reduces infection risk compared to traditional contact-based methods. Future work could expand the algorithm's application by integrating additional physiological parameters beyond heart rate.

A. Clinical Relevance and Future Directions

Our analysis shows that respiration-related movements are detectable across broader regions of the body, while heart-related movements are more localized. This insight suggests that future radar setups could optimize detection by focusing on fewer range bins, ideally within the first 16 range bins closest to the radar sensor. By reducing the number of range bins, device design and costs can be simplified, improving computational efficiency and data processing speed, which is critical for real-time ICU monitoring.

While the algorithm performs well in general heart rate monitoring, future improvements are needed to handle arrhythmic signals, especially for cardiac patients. Due to the nature of autocorrelation, the algorithm inevitably excludes arrhythmic segments to maintain accuracy in regular heart rate detection,

TABLE III: Comparison of recent radar-based methods for heart rate detection.

Study	Radar Type	Data Processing Techniques	Noise Handling Techniques	Subject Type	Error (MAE in bpm)
[11] Xu et al. (2021)	UWB Radar	Harmonic Peak Selection	Respiratory harmonics suppression	Healthy	1.32
[27] Moadi et al. (2024)	FMCW Radar	Generalized Sidelobe Canceller	Dynamic multi-subject tracking	Healthy	2.5
[28] Marty et al. (2024)	FMCW Radar	Frequency Analysis Techniques	Adaptive noise filtering	Healthy	3.0
[29] Lopes et al. (2024)	FMCW Radar	Signal Denoising	Real-time noise management for nursing homes	Elderly	3.2
[30] Li et al. (2024)	FMCW Radar	Efficient Phase Extraction	Optimized for ultra-narrow range monitoring	Healthy	1.3
[31] Hu et al. (2024)	FMCW Radar	Multi-Point Scattering Model	Respiration and heartbeat separation	Healthy	2.1
This Study	FMCW Radar	**Autocorrelation-Based Estimation**	**Periodicity and Amplitude Change-based Filtering**	**Post-surgical ICU**	**2.22**

which currently limits its application for patients with frequent arrhythmias. Implementing techniques such as template matching or adaptive filtering could enhance performance for irregular heart rhythms, supporting ICU staff with a more comprehensive monitoring tool suited to diverse patient care needs.

B. Comparison with Recent Radar-Based Heart Rate Detection Methods

Recent radar-based heart rate monitoring methods have achieved notable advancements in accuracy and noise management. Table III provides a comparative overview of key studies, including radar types, processing techniques, subject groups, and performance metrics. Our study demonstrates an MAE of 2.22 bpm, emphasizing its robustness in ICU settings characterized by patient movement, arrhythmias, and other challenges not often considered in studies focusing on healthy individuals.

Xu et al. (2021) achieved an MAE of 1.32 bpm using a UWB radar positioned directly above the bed. While this setup eliminates obstacles, it is impractical in ICU workflows where overhead equipment can interfere with patient care. Moreover, their focus on healthy subjects might limit the applicability of their results to ICU patients with variable and complex physiological states. Moadi et al. (2024) reported an MAE of 2.5 bpm using a system evaluated under controlled conditions, which may not sufficiently address the noise and variability common in ICU environments.

Marty et al. (2024) placed their FMCW radar in front of the subjects, achieving an MAE of 3.0 bpm. Lopes et al. (2024) positioned their radar on top of the bed and reported an MAE of 3.2 bpm. While both setups are effective for stationary monitoring, neither accounts for challenges such as patient movement or the potential interference from bed frames, which can attenuate signal quality in ICU conditions.

Li et al. (2024) achieved an MAE of 1.3 bpm with a radar placed above the chest of five healthy subjects, while Hu et al. (2024) achieved 2.1 bpm using a radar positioned in front of two seated subjects. Both studies, conducted on small sample sizes in controlled environments, may lack the robustness needed for the dynamic and variable ICU context.

Our system, with its under-bed placement, is designed specifically for ICU use. This unobtrusive configuration minimizes interference with clinical workflows while reliably capturing high-quality signals through potential obstacles like bed frames and mattresses. Additionally, our periodicity- and amplitude-based filtering techniques effectively handle noise, making the system a practical and reliable solution for continuous, non-invasive monitoring in ICU environments.

V. Conclusion

In conclusion, our study introduces a novel radar-based algorithm for heart rate estimation in an ICU setting. The algorithm demonstrated high accuracy and robustness in real-world conditions, effectively handling motion artifacts and patient position changes. This radar-based monitoring system has the potential to enhance patient care in intensive care units by providing continuous, non-invasive monitoring of vital signs, reducing the need for manual measurements, and minimizing patient discomfort. One of the key strengths of this study is its validation on patients recovering from cardiovascular interventions, highlighting the algorithm's applicability in clinical settings.

However, some limitations were noted, particularly in the presence of arrhythmias. The current quality assessment criteria often exclude arrhythmic segments due to their inconsistent and irregular nature, affecting the accuracy of heart rate estimation. Future research should focus on developing more sophisticated algorithms specifically designed to handle such irregularities, ensuring accurate heart rate estimations even in the presence of arrhythmias. These enhancements could include template matching techniques to identify specific patterns associated with different arrhythmia types. Overall, this work lays a solid foundation for future innovations in healthcare technology, with potential applications extending beyond cardiovascular monitoring to other areas of patient care.

Acknowledgment

This study was conducted as part of the Moore4Medical Project (M4M), which received funding from the Electronic Components and Systems for European Leadership Joint Undertaking (ECSEL JU) in collaboration with the European

Union's H2020 Framework Programme (H2020/2014-2020) and National Authorities, under grant agreement H2020-ECSEL-2019-IA-876190. We appreciate the support provided by this initiative in enabling our research.

REFERENCES

[1] Anuradha Singh, S. Rehman, Sira Yongchareon, and P. Chong. Multi-resident non-contact vital sign monitoring using radar: A review. *IEEE Sensors Journal*, 21(4):4061–4084, 2021.

[2] Gregory A Roth et al. Global, regional, and national burden of cardiovascular diseases and risk factors, 1990–2019: update from the gbd 2019 study. *Journal of the American College of Cardiology*, 76(25):2982–3021, 2020.

[3] World Health Organization. Cardiovascular diseases (cvds), 2021.

[4] Giacomo Paterniani, D. Sgreccia, A. Davoli, Giorgio Guerzoni, Pasquale Di Viesti, A. Valenti, M. Vitolo, G. Vitetta, and G. Boriani. Radar-based monitoring of vital signs: A tutorial overview. *Proceedings of the IEEE*, 111(2):277–317, 2023.

[5] Srikrishna Iyer et al. mm-wave radar-based vital signs monitoring and arrhythmia detection using machine learning. *Sensors*, 22(9):3106, 2022.

[6] Mamady Kebe et al. Human vital signs detection methods and potential using radars: A review. *Sensors*, 20(5):1454, 2020.

[7] Gabriel Beltrao et al. Recent developments in contactless monitoring vital signs using radar devices. *arXiv preprint arXiv:2307.09101*, 2023.

[8] John Allen. Photoplethysmography and its application in clinical physiological measurement. *Physiological measurement*, 28(3):R1, 2007.

[9] Yoshiyuki Inoue, Shunsuke Arai, Koji Ogawa, and Hiroyuki Yoshida. Novel bed-integrated ballistocardiography system with high-resolution radar for cardiovascular monitoring in daily living environments. *IEEE Access*, 7:106831–106839, 2019.

[10] Dengyu Qiao, Tan He, Boping Hu, and Ye Li. Non-contact physiological signal detection using continuous wave doppler radar. *Bio-medical materials and engineering*, 24(1):993–1000, 2014.

[11] Hongqiang Xu, M. P. Ebrahim, Kareeb Hasan, F. Heydari, Paul Howley, and M. Yuce. Accurate heart rate and respiration rate detection based on a higher-order harmonics peak selection method using radar non-contact sensors. *Sensors (Basel, Switzerland)*, 22:83, 2021.

[12] Ming-chun Huang, Jason J Liu, Wenyao Xu, Changzhan Gu, Changzhi Li, and Majid Sarrafzadeh. A self-calibrating radar sensor system for measuring vital signs. *IEEE Transactions on Biomedical Circuits and Systems*, 10(2):352–363, 2016.

[13] Changzhi Li, J. Cummings, J. Lam, E. Graves, and Wenhsing Wu. Radar remote monitoring of vital signs. *IEEE Microwave Magazine*, 10(1):47–56, 2009.

[14] Faheem Khan and S. Cho. A detailed algorithm for vital sign monitoring of a stationary/non-stationary human through ir-uwb radar. *Sensors (Basel, Switzerland)*, 17(2):290, 2017.

[15] Anuradha Singh, S. Rehman, Sira Yongchareon, and P. Chong. Multi-resident non-contact vital sign monitoring using radar: A review. *IEEE Sensors Journal*, 21(4):4061–4084, 2021.

[16] S. Schellenberger, Kilin Shi, F. Michler, F. Lurz, R. Weigel, and A. Koelpin. Continuous in-bed monitoring of vital signs using a multi radar setup for freely moving patients. *Sensors (Basel, Switzerland)*, 20(20):5827, 2020.

[17] Giacomo Paterniani, D. Sgreccia, A. Davoli, Giorgio Guerzoni, Pasquale Di Viesti, A. Valenti, M. Vitolo, G. Vitetta, and G. Boriani. Radar-based monitoring of vital signs: A tutorial overview. *Proceedings of the IEEE*, 111(2):277–317, 2023.

[18] André Bourdoux, Marc Bauduin, Kristof Vaesen, Miguel Glassée, Eddy De Greef, Thomas Gielen, and Lija Ocket. A cmos-based 140 ghz 4x4 mimo radar prototype with 10 ghz bandwidth. In *2023 24th International Radar Symposium (IRS)*, pages 1–10, 2023.

[19] G. Beltrão, M. Alaee-Kerahroodi, U. Schroeder, D. Tatarinov, and M. R. Bhavani Shankar. Recent developments in contactless monitoring vital signs using radar devices. *Sensors*, 20(5):1454, 2020.

[20] Malcolm Elliott and Roz Williamson. Is respiratory rate measurement important? an audit of fundamental nursing textbooks. *Medical News Monthly (MNM)*.

[21] Iwona Cygankiewicz and Wojciech Zareba. *Chapter 31 - Heart rate variability*, volume 117 of *Handbook of Clinical Neurology*. Elsevier, 2013.

[22] Mostafa Ghoneim, Ingrid Möller, Georg Jahn, Marius Hellert, and Jan Meyer. Decoding mental effort in a quasi-realistic scenario: A feasibility study on multimodal data fusion and classification. *Sensors*, 20(5):1454, 2020.

[23] Widanalage Dhammika Widanage, John L. Douce, and Keith R. Godfrey. Effects of overlapping and windowing on frequency response function estimates of systems with random inputs. *IEEE Transactions on Instrumentation and Measurement*, 58(1):214–220, 2009.

[24] David P Tadi et al. High-resolution heart rate monitoring using advanced radar technology. *IEEE Transactions on Biomedical Engineering*, 68(4):987–996, 2021.

[25] Ronald W Schafer and Lawrence R Rabiner. Digital signal processing. *IEEE Transactions on Acoustics, Speech, and Signal Processing*, 21(3):123–131, 1973.

[26] Hannu O. Kinnunen. Quality of ambulatory heart rate variability data and artifact correction. Master's thesis, University of Oulu, 1997.

[27] A. K. Moadi, C. Bauder, A. H. Djouadi, P. Theilmann, and A. E. Fathy. Enhancing multi-subject vital sign estimation by utilizing the generalized sidelobe canceller. In *2024 IEEE Topical Conference on Wireless Sensors and Sensor Networks (WiSNeT)*, pages 26–29, 2024.

[28] Steven Marty, Andrea Ronco, Federico Pantanella, Kanika Dheman, and Michele Magno. Frequency matters: Comparative analysis of low-power fmcw radars for vital sign monitoring. *IEEE Transactions on Instrumentation and Measurement*, 73:1–10, 2024.

[29] Sérgio Ivan Lopes, Fábio Silva, Pedro Pinho, Paulo Marques, Carlos Abreu, João Milheiro, Bruno Braga, Gabriel Queirós, Rita Almeida, and Nuno Borges Carvalho. Covis: A contactless health monitoring system for the nursing home. *IEEE Access*, 12:20802–20821, 2024.

[30] Yuchen Li, Keke Zheng, and Changzhan Gu. A fast and efficient fmcw radar phase extraction technique at ultra-narrow range for vital sign detection. In *2024 IEEE/MTT-S International Microwave Symposium - IMS 2024*, pages 1057–1060, 2024.

[31] Yuxuan Hu, Zhaoyang Xia, and Feng Xu. Investigating respiration-heartbeat separation through a multipoint scattering chest wall motion model: 60-ghz fmcw radar assessment. *IEEE Transactions on Instrumentation and Measurement*, 73:1–13, 2024.